Spectrochimica Acta Part B xxx (2008) xxx–xxx

Contents lists available at ScienceDirect

Spectrochimica Acta Part B

journal homepage: www.elsevier.com/locate/sab

# Optimizing total reflection X-ray fluorescence for direct trace element quantification in proteins I: Influence of sample homogeneity and reflector type ☆

G. Wellenreuther [a], U.E.A. Fittschen [b], M.E.S. Achard [a,1], A. Faust [a], X. Kreplin [a], W. Meyer-Klaucke [a,*]

[a] European Molecular Biology Laboratory, Notkestr. 85, 22603 Hamburg, Germany
[b] Department of Chemistry, University of Hamburg, Martin-Luther-King-Platz 6, 20146 Hamburg, Germany

ARTICLE INFO

*Article history:*
Received 1 November 2007
Accepted 8 October 2008
Available online xxxx

*Keywords:*
Metalloprotein
Metal quantification
TXRF
μXRF
Trace elements

ABSTRACT

Total reflection X-ray fluorescence (TXRF) is a very promising method for the direct, quick and reliable multi-elemental quantification of trace elements in protein samples. With the introduction of an internal standard consisting of two reference elements, scandium and gallium, a wide range of proteins can be analyzed, regardless of their salt content, buffer composition, additives and amino acid composition. This strategy also enables quantification of matrix effects. Two potential issues associated with drying have been considered in this study: (1) Formation of heterogeneous residues of varying thickness and/or density; and (2) separation of the internal standard and protein during drying (which has to be prevented to allow accurate quantification). These issues were investigated by microbeam X-ray fluorescence (μXRF) with special emphasis on (I) the influence of sample support and (II) the protein / buffer system used. In the first part, a model protein was studied on well established sample supports used in TXRF, PIXE and XRF (Mylar, siliconized quartz, Plexiglas and silicon). In the second part we imaged proteins of different molecular weight, oligomerization state, bound metals and solubility.
A partial separation of protein and internal standard was only observed with untreated silicon, suggesting it may not be an adequate support material. Siliconized quartz proved to be the least prone to heterogeneous drying of the sample and yielded the most reliable results.



## 1. Introduction

Trace elements are essential for organisms from all kingdoms of life. Pathogenic bacteria compete with their hosts for the limited amounts of essential elements, such as iron [1–3] and control of trace element availability may open new ways to fight bacterial diseases. This however requires an in-depth understanding of the steps involved in trace element homeostasis. Regardless of the great potential of such an approach today only in a limited number of studies accurate quantifications of the trace element content are available. Irrespective of the level, cellular or molecular, this limits future research, because in total, 20 to 30% of all proteins contain metals, either to stabilize protein structures, regulate gene expression, transport electrons or oxygen, induce protein activity or catalyze enzymatic reactions [4].

These days most proteins for research, irrespective of their origin, are expressed in genetically modified bacteria such as *Escherichia coli*. Consequently metal sites are sometimes not correctly assembled, because essential maturation proteins are lacking in *E. coli* [5]. Moreover, the metal contents after isolation can vary from batch to batch in amount and profile. At the same time, for research on isolated proteins the knowledge of type and number of bound metals provides valuable insights: for uncharacterized proteins certain metals can be associated with potential protein functions, which provide a starting point for further studies. For well-known proteins the exact metal profile is essential to interpret biochemical, molecular biology as well as structural data.

To become a routine tool for the determination of protein-bound trace elements an analytical method has to fulfill several requirements:

(1) Sufficient sensitivity to detect metals for a wide range of protein concentrations and protein buffers
(2) Capability of detecting all relevant elements in a single measurement
(3) Requiring as few resources (e.g., time, manpower, money) as possible
(4) Possibility for high sample throughput
(5) Quick measurement and evaluation

A method often used to analyze the elemental composition of protein samples is microbeam Proton Induced X-ray Emission (μPIXE) [4,6–8]. The advantages of μPIXE are its multi-element detection

☆ This paper was presented at the 12th Conference on Total Reflection X-ray Fluorescence Analysis and Related Methods held in Trento (Italy), 18–22 June 2007, and is published in the Special Issue of Spectrochimica Acta Part B, dedicated to that conference.

* Corresponding author. Tel.: +49 4089902124; fax: +49 4089902149.
*E-mail address:* Wolfram@embl-hamburg.de (W. Meyer-Klaucke).
[1] Now at School of Molecular and Microbial Sciences, University of Queensland, Brisbane, Australia.

0584-8547/$ – see front matter © 2008 Elsevier B.V. All rights reserved.
doi:10.1016/j.sab.2008.10.006



Please cite this article as: G. Wellenreuther, et al., Optimizing total reflection X-ray fluorescence for direct trace element quantification in proteins I: Influence of sample homogeneity and reflector type, Spectrochim. Acta Part B (2008), doi:10.1016/j.sab.2008.10.006

capability and the utilization of the protein-intrinsic sulphur standard. Unfortunately, this elegant approach imposes several restrictions on the sample (e.g. protein must contain reasonable number of sulphur atoms, buffer components may not contain any sulphur, chlorine should be replaced by bromine, samples should be thin since the sulphur signal is easily affected by matrix effects). While it is possible to prepare special μPIXE-samples fulfilling these requirements the common denominator for different biochemical, structural and spectroscopic experiments is lost. On the other hand μPIXE is a spatial resolved technique and therefore able to overcome dust contaminations. But due to the scanning process the measurement takes considerable time and its evaluation typically requires expert knowledge.

An alternative to μPIXE is Total Reflection X-ray fluorescence (TXRF) (see [9] and references herein) which already has shown its potential for protein samples [10,11]. This technique allows multi-element detection with a better sensitivity than μPIXE: indeed, its lowest limits of detection (LLDs) are in the order of pg/μl for elements with $Z>18$ (e.g. see Table 5-2 in [9]). Since TXRF is an integrating method, measurements require only a few seconds and easy online data evaluation gives immediate access to most biological relevant trace element concentrations, which allows for high-throughput operation.

In TXRF contaminations (e.g. by dust particles) cannot be directly detected as in μPIXE. Nevertheless their occurrence can be identified by a statistical analysis of the spread of concentrations determined for aliquots of the same sample: Any measurement yielding significantly higher concentrations in a few elements than the others is most probably contaminated, and should be discarded from further evaluation. The utilization of an internal standard, added prior to the TXRF analysis requires the determination of the protein concentration prior to the measurement. The internal standard allows measuring an extremely wide range of protein samples virtually regardless of their buffer, salt concentration or amino acid composition, and hence reduces significantly the time between the protein purification and trace element quantification.

Moreover, access to an X-ray tube-based TXRF-instrument is typically easier than to μPIXE, which requires a proton accelerator. Furthermore, the structural biology community already enjoys broad access to synchrotron radiation facilities, opening the possibility of synchrotron-based TXRF (SR-TXRF) with its advantages of increased flux and high polarization.

The typical protein sample is present in an aqueous solution, which simplifies preparation of samples (as opposed to powdered samples or protein crystals): The sample can be deposited onto a standard TXRF reflector, dried and analyzed. The procedure is simple and the analysis is precise in the presence of an internal standard. This makes TXRF a method of choice, however the homogeneity of dried samples might be critical for an accurate analysis [12,13]. Frequently the presence of salts in mM or M concentration is required to keep a protein in solution. These salts form a major component of the dried residue that will be analysed by TXRF. While drying, components of the sample, either from the buffer, the internal standard or the protein itself, could spatially separate (e.g., due to the formation of salt crystals, "coffee rings" [14] or other aggregation processes). This would affect the thickness of the dried residue, resulting in areas with varying coverage (see Fig. 1) and/or components.

Decomposition of the sample followed by homogenization in liquid could help to circumvent some of these problems, but is not in line with the high-throughput we aim at. Thus an optimized direct method is favoured: (a) sample inhomogeneities are reduced by careful selection of reflector material and surface coating, (b) quantification procedure is developed to determine and quantify matrix effects, and (c) risk of a separation of protein and its metals vs. the internal standard is assessed by micro beam X-ray fluorescence (μXRF) experiments.

The later experiments shed light on the influence of (I) different sample supports and (II) of the protein and the buffer itself on sample homogeneity. For (I) we have chosen Mylar® foil (DuPont, Wilmington (Delaware), USA), siliconized quartz, silicon and Plexiglas as sample supports, since they are being used in a variety of methods, including XRF, μXRF, TXRF and μPIXE. Mylar foils are extensively used as sample supports in μPIXE and XRF since they cause almost no background signal. Quartz reflectors are the standard sample support for TXRF due to their very low surface roughness; but they are quite expensive and we consider their time-consuming re-use as a disadvantage under the aspect of achieving true high-throughput operation. Reflectors made from Plexiglas are cheap enough to be used as single-shot sample supports enabling high-throughput operation. Unfortunately, their surface is rough compared to quartz. This triggered the analysis of silicon wafers: They come with nearly perfect surface quality, and several reflectors can be cut from a single wafer resulting in a potential cost/reflector close to that of Plexiglas. The model protein is a member of the metallo-beta-lactamase super family (hELAC1) from our recent research project [15] which turned out to produce optically inhomogeneous droplets.

To elucidate the influence of the individual protein properties (II) we studied in addition four commercially available metalloproteins of different molecular weight, oligomerization state, bound metals and solubility both on Mylar and siliconized quartz.

## 2. Experimental

### 2.1. Sample preparation

#### 2.1.1. Standard

The X-ray absorption properties of a protein solution depend on a variety of parameters (e.g. protein concentration, concentrations of

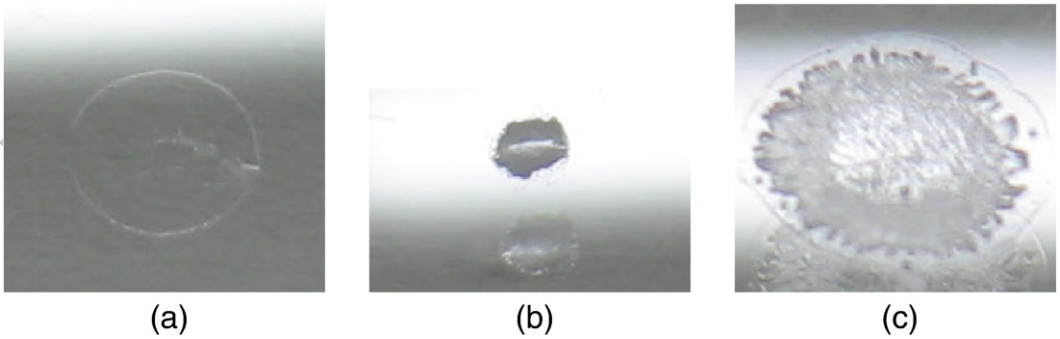


**Fig. 1.** Optical microscopy of dried residues of 10 μL droplets for standard (a), standard + buffer (containing 1% glycerol)(b) and standard + buffer + protein(c) on Plexiglas. While the pure standard dries forming a pronounced "coffee ring", standard + buffer does not completely dry. We attribute this to the hygroscopic effect caused by the glycerol content, which is supported by the fact that any other combination of buffer components lacking glycerol forms thin residue again. Addition of hELAC1 to the buffer containing 1% glycerol also negates the negative effects of glycerol, as hELAC1 is strongly surface active.



Please cite this article as: G. Wellenreuther, et al., Optimizing total reflection X-ray fluorescence for direct trace element quantification in proteins I: Influence of sample homogeneity and reflector type, Spectrochim. Acta Part B (2008), doi:10.1016/j.sab.2008.10.006

buffers / salts / additives) both directly (e.g. affecting the total absorption cross section of the dried solution) and indirectly (e.g. via changed dewetting properties, see Fig. 1). Hence, under high-throughput conditions any protein sample and/or its buffer might exhibit matrix effects. For its quantification we used two internal standards: scandium and gallium, whose $K_\alpha$ fluorescence energies, 4.09 keV and 9.25 keV, differ considerably. Their strong difference in absorption makes it is possible to quantify matrix effects. For example, the transmission of Sc-$K_\alpha$ through 100 μm water (most protein samples predominantly consist of light elements with $Z<18$) is only ~46%, compared to 93.5% of Ga-$K_\alpha$ radiation.

In this work we refer as "standard" a solution containing 10 mg/L of scandium and 1 mg/L of gallium prepared by diluting standard solutions of gallium nitrate and scandium nitrate in 2–3% HNO3 (Merck, Darmstadt standard for ICP-MS) into milliQ water. Adding this standard to the samples to be measured allows us to quantify the amount of matrix effects present in each sample individually, under the assumption that absorption of the Ga fluorescence may be neglected.

### 2.1.2. Purified protein hELAC1

Part I focuses on hELAC1, a Zn-dependent enzyme from the beta-lactamase superfamily; the cloning of the gene and purification of the protein has already been described in one of our previous work [15]. In brief, *hELAC1* was cloned into an expression vector containing an N-terminal His6 tag used for purification and the protein produced by *E. coli* containing this expression vector. The purification of hELAC1 from the bacteria was done in two steps: an affinity chromatography using a nickel-nitrilotriacetate (Ni-NTA) agarose binding the $His_6$ tag of the protein and a gel filtration. At the final step, hELAC1 is pure and solubilized in the buffer used for gel filtration, which contains 20 mM Tris/HCl pH 7.4, 100 mM NaCl, 1% glycerol and 0.5 mM Tris(2-carboxyethyl)phosphine (TCEP). The concentration of purified hELAC1 is determined by measuring the absorption at 280 nm prior to addition of the standard solution. In this study, the concentration of hELAC1 is 15 μM. From now on, we will call "hELAC1" purified hELAC1 sample supplemented with 50% (v/v) of standard and "buffer" gel filtration buffer samples supplemented with 50% (v/v) of standard.

### 2.1.3. Commercially available proteins

The commercially available proteins used in part II were insulin [16,17], concanavalin A [18], thermolysin [18] and glucose isomerase [19] (see Table 1).

Insulin was dissolved in a buffer containing 2 mM $Na_2PO_4$ and 1 mM $Na_3EDTA$. According to the suppliers information the protein powder contains ~0.5% Zn which corresponds to 1 Zn per protein. Concanavalin A (Lectin) was dissolved in milliQ water. Thermolysin, poorly soluble in water, was dissolved in 45% (v/v) dimethyl sulfoxide (DMSO). Glucose isomerase was prepared from a crystal suspension of glucose isomerase by dialysis against milliQ water. The resulting sample was deprived of micro crystals. The natural metal cofactors of glucose isomerase are Mn(II) and Mg(II) but could be substituted by other divalent transition-metal ions [20].

### 2.1.4. Reflectors and sample deposition

The use of nL or even pL droplets has been proposed in order to circumvent problems with spot inhomogeneities [13,21]: While μL droplets may dry inhomogenously, smaller droplets tend to be more homogenous. In addition, nL droplets quickly dry in air, while unassisted drying of μL droplets takes several hours. Increasing the evaporation rate (e.g. by heating or vacuum drying) often causes additional inhomogeneities [13]. This favours nL droplets from the analytical point of view. Quartz reflectors commonly used as sample carriers for TXRF were covered with a silicone layer by pipetting 10 μL of a 10% silicone solution in isopropanol (Serva) onto the reflector and heating at 120 °C for one hour in order to create a hydrophobic surface coating. Mylar foils of 0.6 μm thickness were glued onto aluminium frames. The silicon supports were cut in pieces of 24.7×15.0 mm from a silicon wafer (diameter 200 mm) with the aid of a diamond saw.

Droplets were deposited by the Hydra II Plus One crystallization robot which is part of the high-throughput crystallization facility at EMBL Hamburg (Germany) [18]: The crystallization robot's micro-pipette dispensed single droplets in the middle of each reflector. Droplet volumes can be varied from several μL down to 100 nL. In all μXRF experiments 100 nL droplets were examined. In order to ensure a sufficiently high signal to background ratio for TXRF measurements it was necessary to use 500 nL droplets here. Samples dried within several minutes in covered surroundings to prevent contamination. Thus, drying of the samples is no longer the limiting time factor as opposed to manually preparing samples.

## 2.2. Setup

Both the TXRF as well as the μXRF-measurements were carried out using 18.3 keV X-rays monochromatized by the Ni/C-multilayer system. The TXRF measurements were performed at HASYLAB beamline L (Hamburg, Germany) in a vacuum chamber as described in [22,23]. A peltier-cooled silicon drift detector (VORTEX, SII NanoTechnology, Northridge, USA) with 50 $mm^2$ active area collected emitted fluorescence under an angle of 90° to the incident X-ray beam in plane with the synchrotron. This reduces the scattering background due to the polarization of the incident beam.

For μXRF a polycapillary lens focused the beam down to ~15 μm FWHM [24]. Samples were mounted on a standard x-y-z-translation stage under 45° to both, the incident beam and the fluorescence detector. An optical microscope was included for adjustment and documentation.

## 2.3. Measurements

For TXRF the sample spots on the reflectors were vertically aligned followed by an angle scan to tune into total reflection. TXRF-spectra were taken for 100 s per sample, typically at angles around 30% of the critical angle.

For μXRF the elemental maps were measured on a single droplet considered representative judging from the optical microscope readings. Measuring times per pixel varied from 10 s (for hELAC1 on 3-mm

**Table 1**
Properties of commercial available proteins studied in this work

| | Molecular mass | Bound metals | Oligomeric state | Buffer | Concentration | Obtained from |
|---|---|---|---|---|---|---|
| Insulin [16,17] | 5.7 kDa<br>51 amino acids | 1 Zn per monomer | monomer | 2 mM $Na_2PO_4$<br>1 mM $Na_3EDTA$ | 20 mg/mL | Bovine pancreas<br>(Fluka Cat. No. 57590 Lot. No. S30941 355) |
| Concanava-lin A (Lectin) [18] | 25.6 kDa<br>237 amino acids | Mn | Homo-tetrameric | milliQ water | 25 mg/mL | *Canvalia ensiformis*<br>(Fluka Cat. No. 61760 Lot No. 1142237 10607351) |
| Thermolysin [18] | 37.5 kDa<br>316 amino acids | 1 Zn +<br>4 Ca per monomer | Homo-dimeric | 45% (v/v) dimethyl sulfoxide (DMSO) | 20 mg/mL | *Bacillus thermoproteo-lyticus*<br>(Calbiochem Cat No. 58656, Lot. No. B66938) |
| Glucose isomerase [19] | 43.1 kDa<br>387 amino acids | Natural: Mn(II)+Mg(II),<br>substitutions possible [20] | Homo-tetrameric | milliQ water | 20 mg/mL | *Streptomyces rubiginosus*<br>(Hampton Research Cat. No. HR 7-102 Lot No. 020606) |



Please cite this article as: G. Wellenreuther, et al., Optimizing total reflection X-ray fluorescence for direct trace element quantification in proteins I: Influence of sample homogeneity and reflector type, Spectrochim. Acta Part B (2008), doi:10.1016/j.sab.2008.10.006

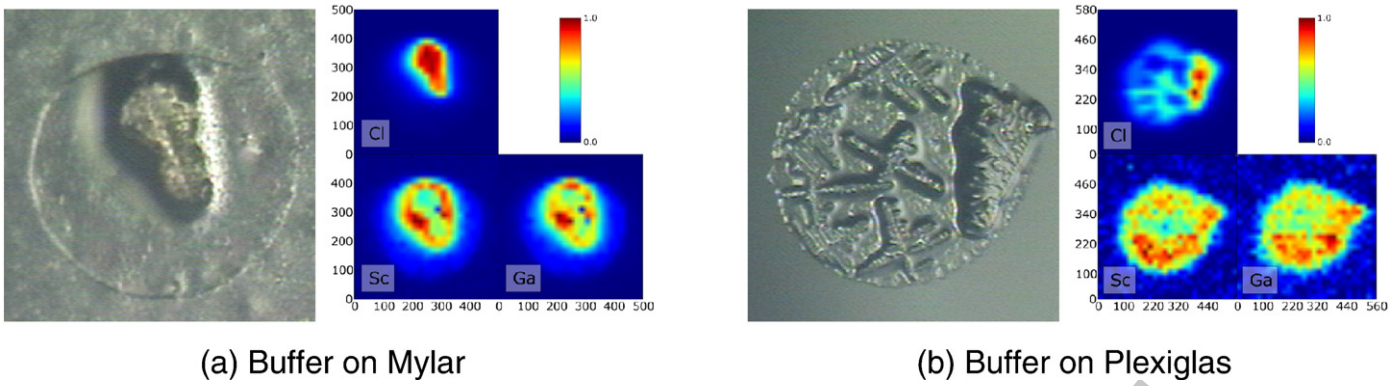


**Fig. 2.** Buffer on Mylar(a) and Plexiglas(b): Comparison of the microscopy images (large image) and elemental maps indicate that crystals containing Cl grow during the drying process.

thick quartz TXRF-reflectors to compensate for the high Compton-scattering background) to less than 1 s (in the case of insulin on Mylar).

### 2.4. Evaluation

TXRF-spectra were fitted with PyMca [25], yielding fluorescence intensities. Taking into account detector efficiencies absolute concentrations were then obtained based on the known Ga standard concentration. In the absence of matrix effects the Sc to Ga ratio as computed by PyMca should match the ratio used during sample preparation (mass ratio Sc:Ga 10 mg/L:1 mg/L, molar ratio 222.4 μM:14.3 μM). Any deviation from these values serves as an estimate for matrix effects.

XRF data were batch-fitted with AXIL [26], yielding raw fluorescence intensities which were used to generate elemental maps. Images were created by mapping the fluorescence intensities to a colour scale. To quantify the homogeneity of the elemental distributions we calculated the Pearson correlation coefficients [27] $c_P$ of two elementals maps

$$c_P(X,Y) = \frac{\mathrm{cov}(\mathrm{map}_X, \mathrm{map}_Y)}{\sigma_X \sigma_Y}$$

with map being the individual elemental maps and $\sigma$ their standard deviation. All correlation coefficients in this work have been calculated with respect to gallium ($Y$=Ga) if not otherwise indicated.

This was applied to circular regions containing only the dried residues. To compare all elemental maps easily, they were scaled to the interval of [0.0,1.0] (only exception Fig. 4d: a very high density of Mn, Sc and Ga in two small salt crystals would otherwise mask the "coffee ring" formation). The figures showing the μXRF results (Figs. 2–4) show elemental maps of Sc and Ga as well as the most important elements



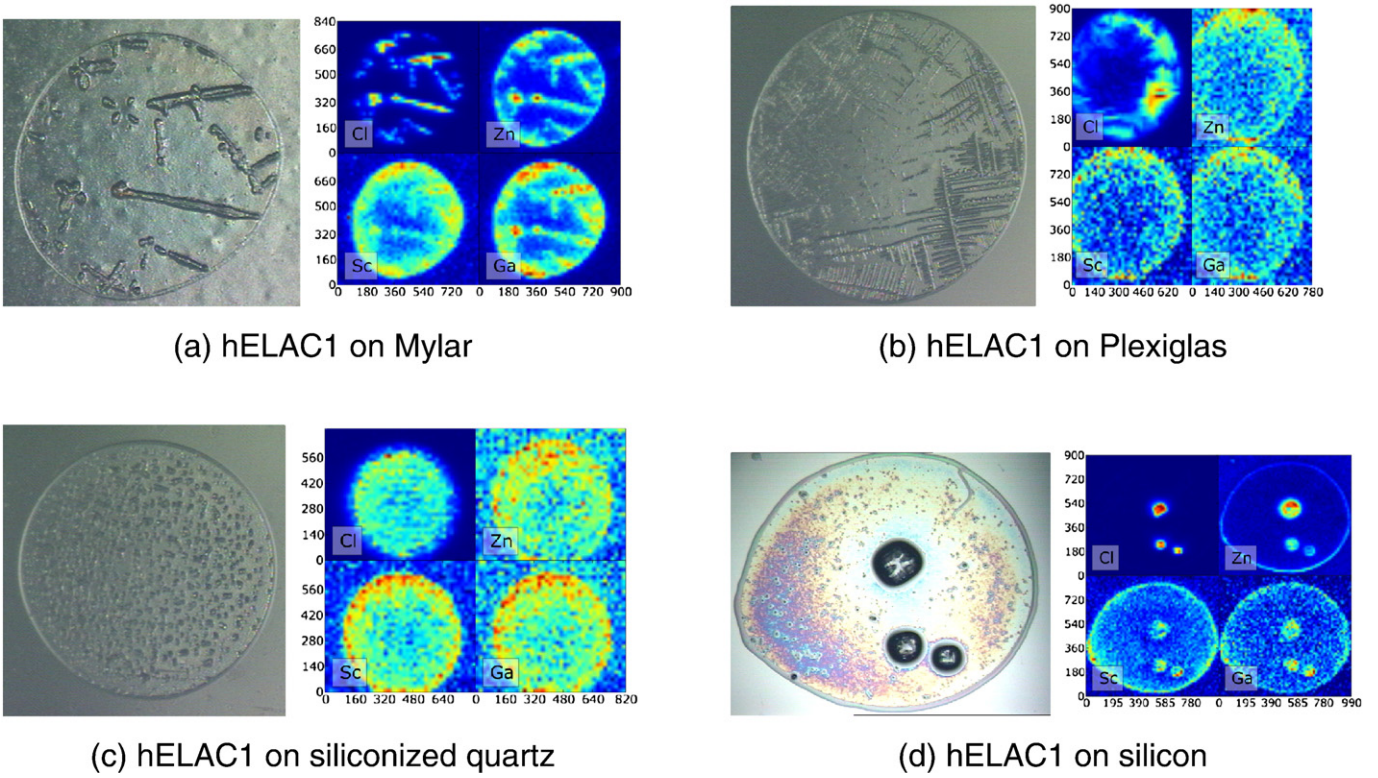


**Fig. 3.** Microscopy and elemental maps of hELAC1 on different reflectors: In the upper row of the elemental maps Cl from the buffer and Zn bound to the protein are shown, while the internal standards Sc and Ga are always shown in the lower row. A colour bar was added for convenience where sufficient space was available. Dimensions of elemental maps are given in μm.

Please cite this article as: G. Wellenreuther, et al., Optimizing total reflection X-ray fluorescence for direct trace element quantification in proteins I: Influence of sample homogeneity and reflector type, Spectrochim. Acta Part B (2008), doi:10.1016/j.sab.2008.10.006

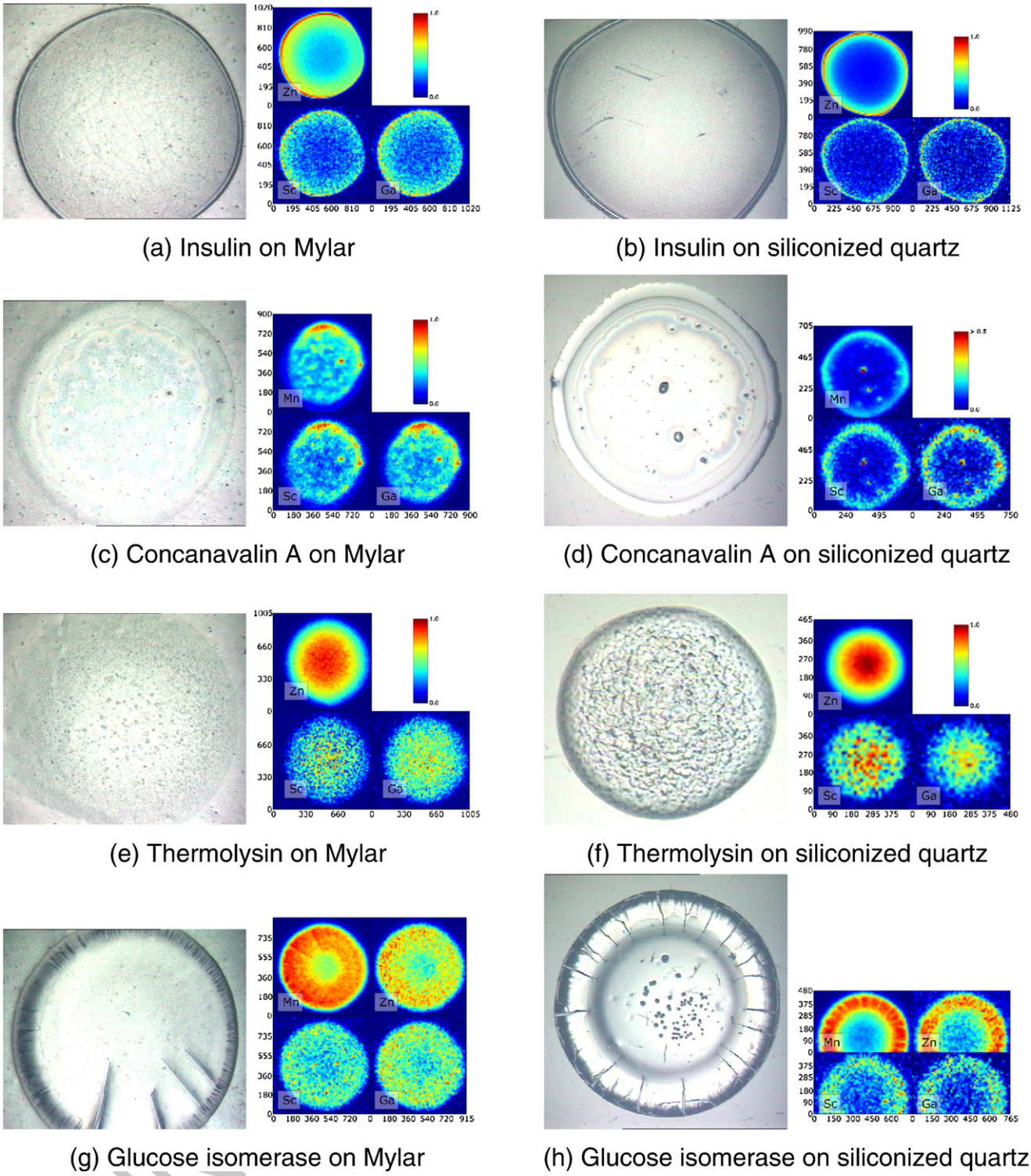


**Fig. 4.** Microscopy and elemental maps of commercially available proteins on Mylar and siliconized quartz: From top to bottom: Insulin, concanavalin A, thermolysin and glucoses isomerase on Mylar (left) and siliconized quartz (right). Despite the observed rich variety of morphologies we observe no evidence for any separation of metals stemming from the proteins compared to Sc or Ga from the internal standard.

for the corresponding sample, e.g. Cl for a buffer, Zn for a Zn-binding protein like Insulin etc.

## 3. Results and discussion

In part I we examined the influence of several sample supports used in analytic methods on the drying properties of a metallo-enzyme (hELAC1) from our most recent study [15]. This is a challenging case because it requires glycerol in the buffer to prevent the loss of catalytic activity upon freezing. But glycerol avoids complete drying, leading to pronounced matrix effects in TXRF. Four different supports were selected (Mylar, siliconized quartz, Plexiglas and silicon wafers) to provide a cross-section of currently-used materials.

In part II we have examined several proteins both on Mylar and siliconized quartz in order to elucidate the influence of the protein properties on the formation of dried residues.

Please cite this article as: G. Wellenreuther, et al., Optimizing total reflection X-ray fluorescence for direct trace element quantification in proteins I: Influence of sample homogeneity and reflector type, Spectrochim. Acta Part B (2008), doi:10.1016/j.sab.2008.10.006

### 3.1. Part I: Shape of dried hELAC1 depends on the reflector type

To address a potential spatial separation of metal stemming from the protein and the (metal) standards Ga and Sc we first had to characterize the metal content of hELAC1 by TXRF.

#### 3.1.1. TXRF

Our previous studies on proteins member of the metallo-beta-lactamase super-family (such as hELAC1) have shown their capability to bind different 3d-metals, in particular iron and zinc, but also manganese and some nickel [15,28,29]. The elements of interest found in as isolated hELAC1 as well as in the buffer and standard are given in Table 2. Although no metals have been added explicitly, the buffer contains 2.2 μM of both Ni and Mn as well as 5.4 μM of Fe according to our TXRF analysis. These concentrations were subtracted from the total metal content found in the hELAC1 protein sample to yield the net amount of protein bound metals, e.g. Fe 21.6 μM and Zn 14.8 μM (see as well the two lower rows in Table 2). Small matrix effects were observed (≤10% for Sc $K_\alpha$); these were neglected since the focus is on the identification of the predominantly bound metals and the potential underestimation of biological important elements such as Mn or Fe is even smaller.

The obtained metal concentrations correlated very well with the protein concentration of 15 μM determined by optical absorption spectroscopy prior to drying of the sample on the TXRF sample holder. Taking into account that metallo-beta-lactamases have a dinuclear metal-binding site we can conclude that, in this sample, the active sites of hELAC1 are dominantly occupied by Fe and Zn.

#### 3.1.2. μXRF

The properties of dried residues depend on the nature of both sample and support. On Plexiglas the dried residues differ considerably for pure standard, buffer and hELAC1 protein samples (see Fig. 1). Similar differences are observed for siliconized quartz, silicone and Mylar which we attribute to the differences in hydrophobicity of their surfaces (data not shown). A potential separation of the individual components was studied by optical microscopy and μXRF. Upon drying on Mylar the *standard* forms quite small circles (~50 μm diameter) without any inhomogeneity (XRF data not displayed). Their small size leads to high areal densities of Sc and Ga, causing the observed matrix effects (Table 2). In contrast, the *buffer* forms droplets of ~500 μm diameter (see Fig. 2(a)+(b)), containing large structures with elevated Cl-content, most probably dominantly sodium chloride crystals. Sc and Ga are incorporated into these structures, but their largest peak intensities are found *around* rather than *inside* them. Judging from the three-dimensional impression of Fig. 2(a) this is caused by increased sample thickness around the putative NaCl-crystals. The correlation between Sc and Ga as quantified by the Pearson correlation coefficient $c_P$ (Table 3) shows no significant separation of the two standard components.

t2.1 **Table 2**
Metal contents in TXRF samples are shown in μM

| | Sc | Mn | Fe | Ni | Zn | Ga (ref) |
|---|---|---|---|---|---|---|
| Standard | 202.3(2) | 0.031(1) | 0.023(1) | 0.044(1) | 0.080(1) | 14.3 |
| Buffer+standard | 196(1) | 2.19(5) | 5.42(6) | 0.40(2) | 2.21(3) | 14.3 |
| Protein+buffer+standard | 211(1) | 6.5(1) | 27.0(2) | 1.65(4) | 17.0(1) | 14.3 |
| Net protein content | – | 4.3(1) | 21.6(2) | 1.25(4) | 14.8(1) | – |

The standard solution (first row) contains traces of metals <0.1 μM. The metal concentrations found in the buffer sample (second row) can therefore be attributed to the gel filtration buffer, and have to be subtracted from the metal concentrations found in the protein sample (third row). The resulting net protein concentrations are displayed in the final row. Matrix effects are ≤10% for Sc (expected value of Sc is 222.4 μM) and therefore were neglected.

**Table 3**
The correlation coefficients with respect to Ga for the pure standard and the buffer sample indicate no separation of Sc and Ga

| | Standard on Mylar | Buffer on Mylar | Buffer on Plexiglas |
|---|---|---|---|
| Cl | | 0.74 | 0.84 |
| Sc | 1.00 | 0.98 | 0.94 |

Microscopy images and elemental maps of *hELAC1* on Mylar, Plexiglas, siliconized quartz and silicon are displayed in Fig. 3(a)–(d), respectively. Typical droplet sizes range from ~700–1000 μm. Their optical appearance is dominated by the rich variety of salt crystals formed on the different substrates.

*On Mylar* (Fig. 3(a)) chlorine is predominantly built into needle-like salt crystals. Protein bound Zn as well as the standards Sc and Ga are incorporated into these crystals and the formation of a "coffee ring" is observed [14]. In perfect agreement with the optical impression the correlation coefficients of Sc and Zn with respect to Ga are close to 1.00, proving almost complete linear correlation between the elemental maps. Obviously standard and protein do not separate. Cl is only correlated with Ga at $c_P$=0.62, most probably caused by its absence in the "coffee ring".

Results are similar for *hELAC1 on Plexiglas* (Fig. 3(b)): needle-like crystals containing Cl, coffee-ring formation for protein bound Zn and the standards. Due to the 45° excitation geometry in μXRF the incident beam penetrates deep into the sample supports, causing elastic and inelastic scattering. While this is negligible for 0.6 μM thick Mylar for all other sample supports scattering caused an increased background. This reduces the signal-to-noise ratio (SNR) significantly, despite a fivefold increase of the data acquisition time per pixel. The decrease of the SNR causes a systematic reduction of all correlation coefficients, e.g. $c_P$ (Sc,Ga) drops from 0.93 (Mylar) down to 0.50, $c_P$ (Zn,Ga) decreases from 0.94 to 0.56. This drop does not dependent on the choice of the standard used for the calculation. In fact, $c_P$(Zn,Sc) dropped also down to 0.50, indicating that this change is purely caused by the increased noise-level in the elemental maps. The similar shifts of $c_P$ (Zn,Ga) vs. $c_P$ (Sc,Ga) indicate that no separation of standard and metal from the protein occurs in the case of hELAC1 on Plexiglas (Table 4). Q1

In the case of *hELAC1 on siliconized quartz* Cl is distributed in hundreds of small crystals (<10 μm) homogenously throughout the dried residue, with the exception of a ~50 μm wide outer ring (Fig. 3(c)). Zn, Sc and Ga are predominantly present in this region, again forming a "coffee-ring". No separation of standard and Zn stemming from the protein can be observed neither by visual inspection of the elemental maps nor by the correlation coefficients.

The last case, *hELAC1 on silicon* is slightly different: While one can observe similar features as before (salt crystal formation with inclusion of other elements and "coffee-ring" formation, see Fig. 3(d)), the elemental maps of Ga and Sc show an increased overall density inside the "coffee-ring", which is not the case for Zn. This is in line with a significantly lower $c_P$(Zn,Ga) compared to $c_P$(Sc,Ga), and therefore resembles the only case in which we have found evidence for (partial) separation of metals from the protein vs. standard.

**Table 4**
The correlation coefficients for hELAC1 on Mylar, Plexiglas and siliconized quartz of Sc and Zn with respect to Ga are comparable, thereby indicating no separation of elements

| | Mylar | Plexiglas | Sil. quartz | Silicon |
|---|---|---|---|---|
| Cl | 0.62 | 0.31 | 0.32 | 0.36 |
| Zn | 0.94 | 0.56 | 0.70 | 0.50 |
| Sc | 0.93 | 0.50 | 0.72 | 0.61 |

In the case of hELAC1 on silicon (last column) the correlation of Zn is decreased with respect to Sc, which could indicate a partial separation.



Please cite this article as: G. Wellenreuther, et al., Optimizing total reflection X-ray fluorescence for direct trace element quantification in proteins I: Influence of sample homogeneity and reflector type, Spectrochim. Acta Part B (2008), doi:10.1016/j.sab.2008.10.006

For most supports standard vs. metal stemming from the protein show a similar distribution. Only in one case (hELAC1 on silicon) a partial separation has happened. Interestingly, the dominating effects governing the distribution of metals / standards are their inclusion into salt crystals and the formation of a "coffee-ring".

The nature of the substrate does significantly influence the morphology of the dried residue, esp. the size and distribution of salt crystals and the diameter of the residue ($d_{quartz} < d_{Mylar} < d_{Plexi} < d_{silicon}$). From the perspective of an analytical method the morphology on quartz is most favourable: (I) Due to the siliconization of the surface the residue has the smallest diameter, which is important in order to fully illuminate the whole droplet with small X-ray beams, e.g. at the synchrotron (SR-TXRF). (II) Moreover, only for this support the drying resulted in the homogenous distribution of small sized salt crystals over the entire area.

### 3.2. Part II: Influence of protein type and its buffer on dried residues

To study the influence of protein properties on the formation of dried residues we analysed protein with low molecular weight (insulin) and high molecular weight (glucose isomerase), with different states of oligomerization (glucose isomerase is homo-tetrameric while thermolysin is homo-dimeric) and with different bound metal ions such as Zn (insulin) or Mn (glucose isomerase). We also investigated the influence of the protein solvent on the drying pattern (organic solvent for thermolysin vs inorganic solvent for the other proteins).

#### 3.2.1. μXRF

Upon drying *Insulin* formed very large dried residues (~1000 μm) on Mylar and siliconized quartz (Fig. 4(a)+(b)). Elemental maps show dominant formation of "coffee-rings". No elemental separation is found, neither in the elemental maps nor judging from the correlation coefficients (see Table 5).

Dried residues from *Concanavalin A* (Fig. 4(c)+(d)) are again dominated by "coffee-ring" formation: Cl can be detected primarily in an outer ring of ~50 μm, while Mn associated with the protein and the standards is present in a second, inner ring. Again no elemental separation is evident.

*Thermolysin* (Fig. 4(e)+(f)) shows a completely different drying behaviour, independent of the substrate: Maximum concentrations are found in the centre for all elements, Ca and Zn associated with the protein as well as the standards. Thermolysin is the only protein examined which required DMSO to stay in solution; we expect that this different buffer causes the unusual drying behaviour. Nevertheless no separation is detected in the elementals maps or the correlation coefficients.

*Glucose Isomerase* (Fig. 4(g)+(h)), the largest protein examined, forms very broad "coffee-rings" (~200–300 μm). Again all elements co-localize on Mylar as well as on siliconized quartz.

This allows summarizing: Despite the different drying properties of the proteins examined in part II there is no evidence for a separation of metals associated with the protein and the standards, for any protein / substrate / buffer combination on Mylar or siliconized quartz.

**Table 5**
The correlation coefficients of Zn and Mn associated with different proteins are comparable to the correlation coefficients obtained for Sc, thereby indicating the lack of separation

| | Insulin | | Concanavalin A | | Thermolysin | | Glucose Isomerase | |
|---|---|---|---|---|---|---|---|---|
| | Mylar | Quartz 04 | Mylar | Quartz 02 | Mylar | Quartz 01 | Mylar | Quartz 03 |
| Mn | | | 0.95 | 0.74 | | | 0.87 | 0.70 |
| Zn | 0.87 | 0.73 | | | 0.86 | 0.91 | 0.85 | 0.69 |
| Sc | 0.77 | 0.60 | 0.92 | 0.72 | 0.64 | 0.79 | 0.74 | 0.52 |

## 4. Conclusions

The drying of protein samples on all supports can lead to the formation of salt crystals but typically not to a separation of an internal standard from the metals stemming from the protein. These effects vary depending on the reflector surface properties, as examined for sample supports typically used in analytical methods like TXRF and μPIXE (Mylar, Plexiglas, siliconized quartz and silicon) for the model protein hELAC1, which is known to form inhomogeneous dried residues. Under no conditions occurred a strong separation of protein and internal standards. Only in one case, hELAC1 on silicon, there is evidence for a small separation. This undesirable feature of silicon surfaces strongly suggests to do further work on siliconized silicon surfaces in order to reduce the affinity of the standard for the surface. Among the other supports all our results slightly favour siliconized quartz: It gives the smallest dried residue diameter, the most homogenous distribution of trace metals and salt crystals and showed no sign of any separation for any of the five proteins examined. Siliconized quartz is in conclusion the sample support of choice reducing sample inhomogeneities to a minimum. Plexiglas is a good alternative, especially for the application of TXRF in high-throughput, or if the detection of Si is important.

Moreover, on Mylar and siliconized quartz the influence of protein properties was studied for insulin, concanavalin A, thermolysin and glucose isomerase, which have different properties regarding e.g. solubility, molecular weight, bound metal and oligomerization state. While the morphology of dried residues varies significantly for the different proteins there was no evidence for a separation of internal standard vs. metal bound by the protein in any protein / reflector combination.

Due to the strong morphologic variations of dried protein samples matrix effects have to be considered. Foremost this requires a possibility to detect and quantify matrix effects; for this purpose we propose the application of two internal standards with at least moderately different Z and fluorescence energies with different absorption properties. The high-Z element is used for the quantification of other elements while the known concentration of the low-Z element allows calculating the occurrence of an average matrix. For proteins Sc and Ga are an ideal choice since they are rarely found in proteins and bracket the most important 3d-metals. The implementation of two internal standards enables us to reliably detect and quantify matrix effects; based on this we can correct for first order matrix effects.

In total we only observed one possible case of separation of standard vs. trace element which can be attributed to the choice of reflector (silicon). Thus the general risk of a separation of internal standard from metals associated with the protein is small and our strategy to optimize the quantification of protein samples works successfully:

(a) Sample inhomogeneities can be reduced by using siliconized quartz sample supports.
(b) Matrix effects can be detected and quantified by implementing two element standards from Sc and Ga. Further, a correction of matrix effects in TXRF based on the assumption a complete lack of separation seems feasible.
(c) The risk of a separation of elements of the internal standard vs. metals stemming from the sample is small; apart from matrix effects the remaining influence of the strong variance of dried protein morphologies caused by salt crystal and "coffee ring" formation on the quantification of trace elements is negligible.

Preparation of protein samples using Sc and Ga as internal standards is therefore straightforward, which allows benefiting from the analytical power of TXRF for metalloproteins. Elaborate sample decomposition is not necessary in general; instead a direct analysis of protein samples is feasible.



Please cite this article as: G. Wellenreuther, et al., Optimizing total reflection X-ray fluorescence for direct trace element quantification in proteins I: Influence of sample homogeneity and reflector type, Spectrochim. Acta Part B (2008), doi:10.1016/j.sab.2008.10.006

## Acknowledgements

We gratefully acknowledge support by Gerald Falkenberg at beamline L, HASYLAB. We thankfully acknowledge the financial support from the European Union for BIOXHIT, contract number LSHG-GT 2003-503420.

## References

[1] E. Pohl, J.C. Haller, A. Mijovilovich, W. Meyer-Klaucke, E. Garman, M.L. Vasil, Architecture of a protein central to iron homeostasis: crystal structure and spectroscopic analysis of the ferric uptake regulator, Mol. Microbiol. 47 (2003) 903–915.

[2] M.A. Fischbach, H.N. Lin, D.R. Liu, C.T. Walsh, How pathogenic bacteria evade mammalian sabotage in the battle for iron, Nat. Chem. Biol. 2 (2006) 132–138.

[3] M.E. Schaible, S.H.E. Kaufmann, Iron and microbial infection, Nat. Rev. Microbiol. 2 (2004) 946–953.

[4] H. Natal da Luz, D. Spemann, W. Meyer-Klaucke, W. Troger, Analysis of proteins by particle induced X-ray emission, Nucl. Instr. Meth. B 231 (2005) 308–314.

[5] R. Lill, U. Mühlenhoff, Maturation of iron–sulfur proteins in eukaryotes: mechanisms, connected processes, and diseases, Ann. Rev. Biochem. 77 (2008) 669–700.

[6] E. Garman, Leaving no element of doubt: analysis of proteins using microPIXE, Struct. Fold. Des. 7 (1999) R291–299.

[7] E.F. Garman, G.W. Grime, Elemental analysis of proteins by microPIXE, Prog. Biophys. Mol. Biol. 89 (2005) 173–205.

[8] A. Vogel, O. Schilling, M. Niecke, J. Bettmer, W. Meyer-Klaucke, ElaC encodes a novel binuclear zinc phosphodiesterase, J. Biol. Chem. 277 (2002) 29078–29085.

[9] R. Klockenkämper, Total-Reflection X-ray Fluorescence Analysis, John Wiley & Sons, Inc., 1997

[10] T. Buhrke, S. Löscher, O. Lenz, E. Schlodder, I. Zebger, L.K. Andersen, P. Hildebrandt, W. Meyer-Klaucke, H. Dau, B. Friedrich, M. Haumann, Reduction of unusual iron–sulfur clusters in the H2-sensing regulatory Ni–Fe hydrogenase from Ralstonia Eutropha H16, J. Biol. Chem. (2005) 19488–19495.

[11] D. Barthelme, U. Scheele, S. Dinkelaker, A. Janoschka, F. MacMillan, S.-V. Albers, A.J.M. Driessen, M.S. Stagni, E. Bill, W. Meyer-Klaucke, V. Schunemann, R. Tampe, Structural organization of essential iron–sulfur clusters in the evolutionarily highly conserved ATP-binding cassette protein ABCE1, J. Biol. Chem. 282 (2007) 14598–14607.

[12] L. Fabry, S. Pahlke, L. Kotz, Accurate calibration of TXRF using microdroplet samples, Fresenius' J. Anal. Chem. 354 (1996) 266–270.

[13] T.C. Miller, G. Havrilla, Nanodroplets: a new method for dried spot preparation and analysis, X-Ray Spectrom. 33 (2004) 101–106.

[14] R.D. Deegan, O. Bakajin, T.F. Dupont, G. Huber, S.R. Nagel, T.A. Witten, Capillary flow as the cause of ring stains from dried liquid drops, Nature 389 (1997) 827–829.

[15] M.E.S. Achard, G. Wellenreuther, B. Kostelecky, U.E.A. Fittschen, W. Meyer-Klaucke, Zn is not the only metal activating the Escherichia coli enzyme ElaC and its human homologue ELAC1, both member of the metallo-ß-lactamase superfamily, submitted (2007).

[16] I. Dix, M. Sevvana, G. Bunkóczi, J.É. Debreczeni, G.M. Sheldrick, The EU BIOXHIT standard test crystal, Acta Cryst. A 61 (2005) C147.

[17] E. Hough, L.K. Hansen, B. Birknes, K. Jynge, S. Hansen, A. Hordvik, C. Little, E. Dodson, Z. Derewenda, High-resolution (1.5 A) crystal structure of phospholipase C from *Bacillus cereus*, Nature 338 (1989) 357–360.

[18] J. Mueller-Dieckmann, The open-access high-throughput crystallization facility at EMBL Hamburg, Acta Crystallogr., D 62 (2006) 1446–1452.

[19] H.L. Carrell, J.P. Glusker, V. Burger, F. Manfre, D. Tritsch, J.F. Biellmann, X-ray-analysis of D-xylose isomerase at 1.9 a—native enzyme in complex with substrate and with a mechanism-designed inactivator, Proc. Natl. Acad. Sci. U. S. A. 86 (1989) 4440–4444.

[20] U.A. Ramagopal, M. Dauter, Z. Dauter, SAD manganese in two crystal forms of glucose isomerase, Acta Crystallogr., D 59 (2003) 868–875.

[21] L. Redecke, M.v. Bergen, J. Clos, P.V. Konarev, D.I. Svergund, U.E.A. Fittschen, J.A.C. Broekaert, O. Bruns, D. Georgieva, E. Mandelkow, N. Genov, C. Betzel, Structural characterization of ß-sheeted oligomers formed on the pathway of oxidative prion protein aggregation in vitro, J. Struct. Biol. 157 (2006) 308–320.

[22] G.P.C. Streli, P. Wobrauschek, C. Jokubonis, G. Falkenberg, G. Zaray, A new SR-TXRF vacuum chamber for ultra-trace analysis at HASYLAB, Beamline L, X-Ray Spectrom. 34 (2005) 451–455.

[23] C. Streli, G. Pepponi, P. Wobrauschek, C. Jokubonis, G. Falkenberg, G. Záray, J. Broekaert, U.E.A. Fittschen, B. Peschel, Recent results of Synchrotron radiation induced TXRF at HASYLAB, Beamline L, Spectrochim. Acta Part B 61 (2006) 1129–1134.

[24] G. Falkenberg, O. Clauss, A. Swiderski, T. Tschentscher, Upgrade of the X-ray fluorescence beamline at HASYLAB/DESY, X-Ray Spectrom. 30 (2001) 170–173.

[25] V.A. Sole, E. Papillon, M. Cotte, P. Walter, J. Susini, A multiplatform code for the analysis of energy-dispersive X-ray fluorescence spectra, Spectrochim. Acta Part B 62 (2007) 63–68.

[26] B. Vekemans, K. Janssens, L. Vincze, F. Adams, P.V. Espen, Analysis of X-ray spectra by iterative least squares (AXIL): New developments, X-Ray Spectrom. 23 (1994) 278–285.

[27] J.R. Green, Statistical Treatment of Experimental Data, Elsevier, 1978.

[28] O. Schilling, N. Wenzel, M. Naylor, A. Vogel, M. Crowder, C. Makaroff, W. Meyer-Klaucke, Flexible metal binding of the metallo-beta-lactamase domain: Glyoxalase II incorporates iron, manganese, and zinc in vivo, Biochemistry 42 (2003) 11777–11786.

[29] N.F. Wenzel, A.L. Carenbauer, M.P. Pfiester, O. Schilling, W. Meyer-Klaucke, C.A. Makaroff, M.W. Crowder, The binding of iron and zinc to glyoxalase II occurs exclusively as di-metal centers and is unique within the metallo-beta-lactamase family, J. Biol. Inorg. Chem. 9 (2004) 429–438.

Q2



Please cite this article as: G. Wellenreuther, et al., Optimizing total reflection X-ray fluorescence for direct trace element quantification in proteins I: Influence of sample homogeneity and reflector type, Spectrochim. Acta Part B (2008), doi:10.1016/j.sab.2008.10.006